Developmental Cell
Article

# DRE-1: An Evolutionarily Conserved F Box Protein that Regulates *C. elegans* Developmental Age

Nicole Fielenbach,[1] Daniele Guardavaccaro,[2] Kerstin Neubert,[3] Tammy Chan,[1] Dongling Li,[1] Qin Feng,[1] Harald Hutter,[4] Michele Pagano,[2] and Adam Antebi[1,*]
[1] Baylor College of Medicine, Huffington Center on Aging, Department of Molecular and Cellular Biology, One Baylor Plaza, Houston, TX 77030, USA
[2] Department of Pathology, NYU Cancer Institute, NYU School of Medicine, 550 First Avenue, MSB 599, New York, NY 10016, USA
[3] Max-Planck-Institut fuer Molekulare Genetik, Ihnestrasse 73, 14195 Berlin, Germany
[4] Department of Biological Sciences, Simon Fraser University, Burnaby, British Columbia V5A 1S6, Canada
*Correspondence: aantebi@bcm.edu
DOI 10.1016/j.devcel.2007.01.018

## SUMMARY

**During metazoan development, cells acquire both positional and temporal identities. The *Caenorhabditis elegans* heterochronic loci are global regulators of larval temporal fates. Most encode conserved transcriptional and translational factors, which affect stage-appropriate programs in various tissues. Here, we describe *dre-1,* a heterochronic gene, whose mutant phenotypes include precocious terminal differentiation of epidermal stem cells and altered temporal patterning of gonadal outgrowth. Genetic interactions with other heterochronic loci place *dre-1* in the larval-to-adult switch. *dre-1* encodes a highly conserved F box protein, suggesting a role in an SCF ubiquitin ligase complex. Accordingly, RNAi knockdown of the *C. elegans* SKP1-like homolog SKR-1, the cullin CUL-1, and ring finger RBX homologs yielded similar heterochronic phenotypes. DRE-1 and SKR-1 form a complex, as do the human orthologs, hFBXO11 and SKP1, revealing a phylogenetically ancient interaction. The identification of core components involved in SCF-mediated modification and/or proteolysis suggests an important level of regulation in the heterochronic hierarchy.**

## INTRODUCTION

Animal development occurs as a succession of life stages, often punctuated by dramatic transitions such as metamorphosis or puberty. The stereotyped course of developmental events suggests that a species life plan is genetically programmed, but the molecular basis is largely unknown. Pioneering work in the nematode *C. elegans* has identified the heterochronic genes as key regulators of temporal programming (Ambros and Horvitz, 1984; Chalfie et al., 1981; Rougvie, 2005). *C. elegans* develops from embryo to adult through four larval stages, L1–L4, each marked by ecdysis. Every stage has a characteristic constellation of stage-specific events, as revealed by the complete description of development (Sulston and Horvitz, 1977; Sulston et al., 1983). Invariant cellular and morphogenetic programs form a precise framework for seeing changes in the relative timing of developmental events.

The *C. elegans* heterochronic loci specify the temporal identity of stage-specific programs (Rougvie, 2005). Mutants result in precocious or delayed development in particular tissues, causing programs to be expressed at earlier or later larval stages. At the cellular level, programs are often repeated or deleted, with little or no effect on molting per se. Most identified loci are transcriptional or translational regulators, many of which are remarkably conserved, including the first discovered microRNAs (Lagos-Quintana et al., 2002; Lee et al., 1993; Pasquinelli et al., 2000; Reinhart et al., 2000; Wightman et al., 1993).

The heterochronic genes comprise a genetic hierarchy, whose regulatory interactions orchestrate postembryonic development (Rougvie, 2005). This hierarchy has been largely elucidated in extragonadal tissues, specifically within epidermal seams (Ambros, 1989), which are lateral midline cells that undergo asymmetric stem cell division patterns during larval development with stage-specific variations (Sulston and Horvitz, 1977). Early larval development is established by LIN-14, a nuclear protein (Ambros and Horvitz, 1984; Ruvkun and Giusto, 1989), and LIN-28, a conserved RNA-binding protein (Moss et al., 1997), which inhibit late larval programs, and thereby specify L1/L2 temporal fates. Their downregulation by the *lin-4*/microRNA (Lee et al., 1993; Wightman et al., 1993) advances programs to the L3 fate. Nuclear hormone receptor DAF-12/NHR (Antebi et al., 2000), the LIN-46/gephyrin homolog (Pepper et al., 2004), as well as microRNAs *mir-84*, *mir-48*, and *mir-241* (*let-7* sisters) cooperate to specify the L2/L3 transition, in part by downregulation of HBL-1/hunchback (Abbott et al., 2005; Li et al., 2005).

Late in development, circadian rhythm homologs LIN-42/period, TIM-1/timeless, and KIN-20/doubletime (Banerjee et al., 2005; Jeon et al., 1999), as well as

HBL-1/hunchback (Abrahante et al., 2003; Lin et al., 2003) and LIN-41/RBCC (Slack et al., 2000), prevent expression of LIN-29/Zn finger transcription factor (Rougvie and Ambros, 1995), thereby specifying L4 fates. Finally, down-regulation of LIN-41 by *let-7*/microRNA (Reinhart et al., 2000; Slack et al., 2000), as well as HBL-1 by *let-7* and its sisters (Abbott et al., 2005), ultimately derepresses LIN-29/Zn finger transcription factor, which specifies the larval-to-adult (L/A) switch (Ambros, 1989).

Other tissues besides the epidermis, including neurons (Abrahante et al., 2003; Hallam and Jin, 1998; Lin et al., 2003), intestine, and vulva (Ambros and Horvitz, 1984; Antebi et al., 1998), are regulated by the heterochronic loci, but the timing circuits in these tissues are not as well understood. Moreover, most identified heterochronic regulators have little obvious impact on gonadal development (Rougvie, 2005), reflecting a fundamental division between gonad and soma, with important developmental and perhaps evolutionary implications.

DAF-12, a nuclear receptor homologous to vertebrate vitamin D and liver-X receptors dictates both gonadal and extragonadal developmental age (Antebi et al., 1998, 2000). The most striking aspect of somatic gonadal development is outgrowth of the gonad, led by the hermaphrodite distal tip cells (dtcs) and male linker cell, which undergo stage-specific migrations. In *daf-12* ligand-binding domain (LBD) mutants, the dtcs fail their L3 turns and repeat L2 longitudinal migration programs instead (Antebi et al., 1998). Similarly, in extragonadal tissues such as epidermis and intestine, mutants repeat L2-specific patterns of cell and nuclear division. A simple idea is that DAF-12 coordinates L3 programs throughout the body via a hormonal mechanism, a notion supported by the identification of hormone biosynthetic genes (Gerisch et al., 2001; Jia et al., 2002; Rottiers et al., 2006) and bile acid-like ligands (Held et al., 2006; Motola et al., 2006). DAF-12 is also essential for the L3 dauer diapause, a long-lived arrested developmental stage.

*daf-12*'s heterochronic function is nonessential, since the phenotypes of null mutants are impenetrant. This implies that stage selectors work in a regulatory network rather than a strict linear pathway. To obtain *daf-12* parallel functions, we focused on enhancers of gonadal heterochrony, and we identified an evolutionarily conserved F box protein that regulates developmental age in gonadal and extragonadal tissues. Its molecular identity implies a role in SCF-mediated protein modification or degradation, suggesting an important level of control in the heterochronic circuits.

## RESULTS

### *dre-1* Mutants Display Gonadal Outgrowth Defects

Morphogenesis of the hermaphrodite gonad is guided by stage-specific migrations of the two dtcs. First located at the ventral midbody, the dtcs move oppositely toward head and tail during L2, then migrate dorsally and centripetally during L3, and finally meet back at the dorsal midbody during L4 and halt (Figures 1AI and 1B). The nuclear receptor *daf-12* influences L3 migrations. *daf-12* nulls (e.g., *rh61rh411*), with lesions in DNA and ligand-binding domains (Antebi et al., 1998, 2000), display little or no migration defects (Figure 1D). However, gain-of-function mutants with lesions in the LBD only (e.g., *rh61*), render *daf-12* a constitutive repressor, and fail their turns (Mig phenotype, Figures 1AII and 1F), interpreted as a heterochronic delay in L3 path-finding programs. The impenetrant heterochronic phenotypes of *daf-12* nulls suggest parallel functions, while the stronger phenotypes of *daf-12(rh61)* are proposed to arise from inhibition of these parallel functions at the promoters of shared target genes (Antebi et al., 2000; Ludewig et al., 2004).

To obtain postulated *daf-12* parallel functions, we screened for Syn-Mig mutants (synthetic migration phenotype) that showed enhanced gonadal heterochrony in the *daf-12(rh61rh411)* null background (see Experimental Procedures). We obtained eight alleles of *dre-1* (for *daf-12* redundant function). *dre-1;daf-12* double mutants displayed penetrant Syn-Mig phenotypes in which the dtcs failed to reflex during L3 (Figures 1AII–1AIV and 1E; Table 1; Table S1, see the Supplemental Data available with this article online), similar to *daf-12(rh61)* (Figure 1F). Furthermore, Syn-Mig phenotypes were not allele specific, since other *daf-12* loss-of-function alleles (e.g., *sa156*) as well as *daf-12(RNAi)* elicited the same phenotype when combined with *dre-1(dh99)* (Table S1; data not shown). Alone, *dre-1* mutants exhibited impenetrant defects, in which the dtcs failed to migrate completely back to the midbody (Figure 1C). Finally, gonadal outgrowth defects of *dre-1(dh99);daf-12(rh61)* doubles were not more severe than those of *rh61* alone (data not shown), suggesting that these mutants impact functionally related pathways.

### *dre-1* Displays Precocious Epidermal Differentiation

Positioned along the lateral midline, epidermal seam cells undergo asymmetric stem cell divisions at each larval stage. During L4, at the L/A transition, seam cells exit the cell cycle, fuse into a long syncitium, and synthesize a continuous ridged cuticular structure, called adult alae, which serve as specific markers of the adult fate. Consistent with a role in developmental timing, *dre-1(dh99)* exhibited precocious fusion of seam cells (85% of animals, Table 2) one stage early prior to the L3 molt (L3m), as visualized with *ajm-1::gfp* (Figures 2A and 2B). Under Nomarski optics, a fraction of animals (15%) also faintly displayed precocious adult alae (Figures 2D and 2E; Table 2). At the L4m, half of the animals had gaps in the adult alae (Figures 2G and 2H; Table 2), a phenotype that can arise in either delayed or precocious heterochronic mutants (Ambros and Horvitz, 1984; A.A., unpublished data). Closer inspection suggested precocious behavior, since seam cells lying beneath the gap had ceased division (data not shown). Like many other heterochronic loci, epidermal phenotypes were suppressed when animals developed through the dauer stage (Table 2) (Liu and Ambros, 1989). Altogether, these phenotypes suggest that *dre-1* regulates the L/A switch in the epidermis.

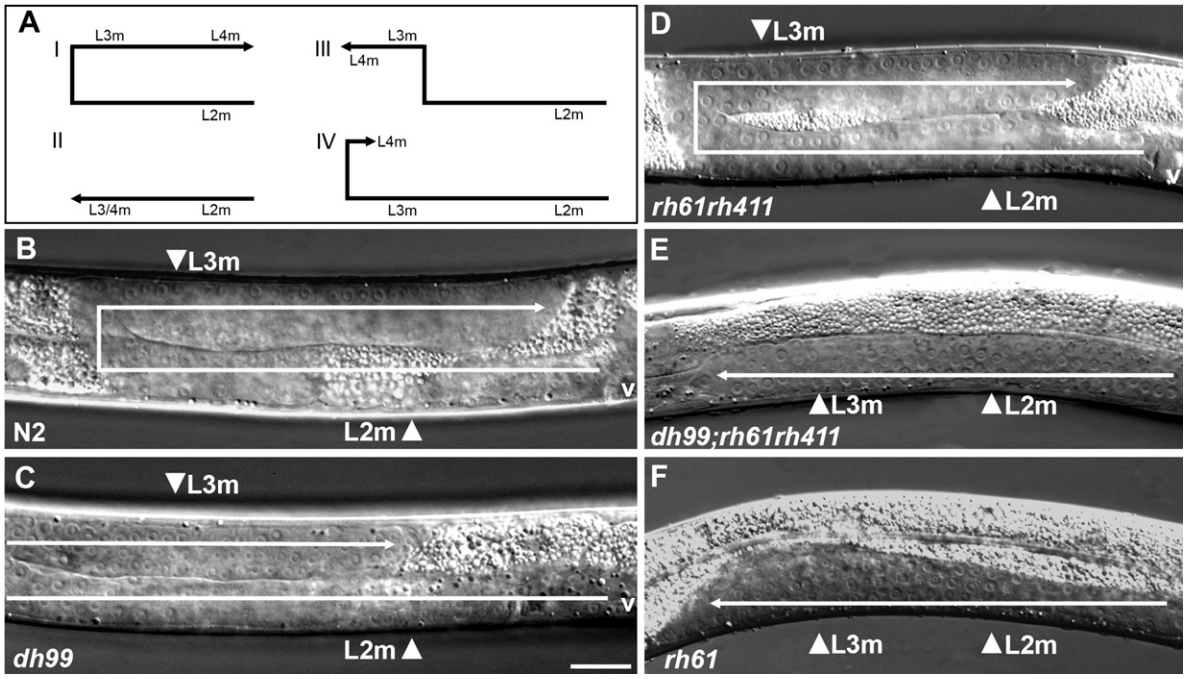


**Figure 1. Gonadal Mig Phenotypes of Late L4 Animals**

(A) Schematic of gonadal migration of wild-type and mutants. I, wild-type (WT); II, errors in both dorsal and centripetal turns; III, error in the centripetal turn; IV, delayed dorsal and centripetal turns.

(B) Normal reflexion of WT N2 gonadal arms.

(C) Impenetrant migration defects of *dre-1(dh99)*.

(D) Normal reflexion of *daf-12(rh61rh411)* null mutants.

(E) Unreflexed gonadal arms of *dre-1(dh99);daf-12(rh61rh411)*.

(F) Unreflexed gonadal arms of *daf-12(rh61)*.

The left gonadal arm of late L4 animals is depicted. Arrowheads indicate the position of the dtcs at the molts. The L4m position is not shown because the dtcs have not reached their final destinations. V, vulva. The scale bars are 10 μm.

### *dre-1* Genetic Interactions for Epidermal Heterochrony

To further analyze the role of *dre-1* in the L/A transition, we performed epistasis experiments with delayed mutants and synergy experiments with precocious mutants. For epidermal phenotypes, we examined seam cell fusion and/or adult alae formation at the L3m and L4m. *lin-29*/Zn finger is the ultimate regulator of the L/A switch. In null mutants, seam cell fusion and adult alae formation fail to occur with complete penetrance (Ambros, 1989; Rougvie and Ambros, 1995). As expected, in *dre-1;lin-29* double mutants, *lin-29* delayed phenotypes prevailed, placing *dre-1* upstream (Table 2). The *let-7*/microRNA triggers the L/A switch by downregulating *lin-41*/RBCC, thus permitting *lin-29* expression (Reinhart et al., 2000; Slack et al., 2000). Null mutants display incomplete seam cell fusion, little or no adult alae, and lethal bursting at the L4m. In *dre-1;let-7* animals, *dre-1* precocious phenotypes largely prevailed. Over half of the animals displayed seam cell fusion at the L3m (Table 2), adult alae at the L4m (although faint and incomplete), and reduced lethal bursting (from 98% down to 73%, n = 300). Thus, *dre-1* works downstream or parallel to *let-7*. *lin-46*/gephyrin specifies L3 and later temporal fates (Pepper et al., 2004). Mutants repeat L2 division patterns at the L3 stage, which results in alae gaps at the L4m. At the L3m, *lin-46* suppressed *dre-1* precocious seam cell fusion, suggesting that at this stage *dre-1* works upstream of *lin-46*. At the L4m, *dre-1;lin-46* animals exhibited normal adult alae (Table 2). This mutual suppression suggests that, at this stage, they work in parallel. Like *lin-46*, *daf-12* null mutants also repeat L2 division patterns at the L3 stage with incomplete penetrance (Antebi et al., 1998). However, in *dre-1;daf-12* double mutants, animals displayed precocious fusion and an alae gap phenotype similar to those of *dre-1* alone, suggesting that *dre-1* works downstream or parallel to *daf-12*. Finally, the *lin-4*/microRNA triggers the L1/L2 transition. Mutants repeat L1 programs at subsequent stages and never express adult programs (Ambros and Horvitz, 1984). In *dre-1;lin-4* doubles, the *lin-4* phenotypes prevailed: seam fusion and adult alae formation were not seen, consistent with a later function for *dre-1* (Table 2).

Several components of the L/A switch, including *lin-41*/RBCC and *hbl-1*/hunchback, exhibit impenetrant precocious phenotypes at the L3m that are attributed to parallel pathways and are revealed by genetic synergy (Abrahante et al., 2003; Lin et al., 2003). *lin-41(RNAi)* animals showed

**Table 1. Gonadal Mig Phenotypes**

| Genotype | % Gonadal Reflexion at L3m[a] | % Gonadal Reflexion at L2m[b] |
|---|---|---|
| N2 | 100 | 0 |
| *dre-1(dh99)* | 100 | 0 |
| *dre-1(dh99)* on L4440 | 100[c] | nd |
| *dre-1(dh99)* on *dre-1(RNAi)* | 100[c] | nd |
| *daf-12(rh61rh411)* | ≥99 | 0 |
| *daf-12(rh61)* | 0 | nd |
| *dre-1(dh99);daf-12(rh61rh411)* | 4 | nd |
| *daf-9(k182)* | 95 | nd |
| *daf-9(k182);dre-1(dh99)* | 30 | nd |
| *daf-36(k114)* | 100 | nd |
| *daf-36(k114);dre-1(dh99)* | 22 | nd |
| *lin-29(n546)* | 100 | nd |
| *lin-29(n546);dre-1(dh99)* | 0 | nd |
| *lin-29(n546);daf-12(rh61rh411)* | 8 | nd |
| *dre-1(dh99);daf-12(rh61rh411); lin-29(RNAi)* | 0 | nd |
| *lin-42(RNAi)* | 100 | 44 |
| *dre-1(dh99);lin-42(RNAi)* | 100 | 10 |
| *daf-12(rh61rh411);lin-42(RNAi)* | 94 | 9 |
| *dre-1(dh99);daf-12(rh61rh411); lin-42(RNAi)* | 34 | 5 |

n ≥ 40 gonad arms (≥20 animals); nd, not determined. Animals were grown at 20°C. RNAi was performed by feeding, except *lin-42(RNAi)*, which was injected. Experiments were performed at least twice.

[a] Percentage of hermaphrodite dtcs that reflexed normally around the L3m. Animals were scored at ages between L3m and L4m, and reflexion was inferred from the final gonadal trajectory.

[b] Percentage of hermaphrodite dtcs that reflexed precociously at the L2m.

[c] Gonadal arms reflexed at the L3m, but failed to fully migrate back toward the midbody. *dre-1(dh99)* on L4440, 20%; *dre-1(dh99)* on *dre-1(RNAi)*, 40%.

precocious adult alae of good quality, but only a fraction of cells (27%) displayed the phenotype (Table 2). In *dre-1;lin-41* doubles, these phenotypes were strongly enhanced, since all seam cells gave rise to high-quality precocious alae. Alone, *hbl-1(RNAi)* elicited penetrant, precocious adult alae formation at the L3m, but the alae were of lower quality. In contrast to *lin-41*, *dre-1* only weakly enhanced *hbl-1* phenotypes (Table 2).

### *dre-1* Genetic Interactions for Gonadal Heterochrony

Most identified heterochronic loci have no obvious gonadal Mig defects. We surmised that underlying roles might be masked by functional redundancy, which could be revealed in synergistic interactions. We therefore made double mutants of *daf-12* and *dre-1* with all other known loci, by using either mutants or RNAi. First, we saw Syn-Mig phenotypes in *dre-1* with *daf-36(k114)*/Rieske oxygenase and *daf-9(k182)*/cytochrome P450 mutants (Table 1), which impair DAF-12 ligand production (Gerisch et al., 2001; Rottiers et al., 2006), showing that reduction of receptor activation produces Mig defects. Intriguingly, we also found that *dre-1;lin-29* and *daf-12;lin-29* double mutants gave strong Syn-Mig phenotypes, in which the dtcs failed one or both turns (Figures 1AII–1AIV; Table 1). Moreover, in *daf-12;dre-1;lin-29* triple mutants, the dtcs invariably failed both turns, resembling *daf-12(rh61)* (Figure 1II; Table 1). Therefore, these loci together promote gonadal reflexion during L3.

RNAi of *lin-42*/period leads to precocious reflexion one stage earlier at the L2m (Tennessen et al., 2006). As reported, we found that *lin-42(RNAi)* injected into wild-type induced precocious gonadal turns at the L2m in 44% of animals. *dre-1*, *daf-12* null, or *dre-1;daf-12* double mutants partially suppressed precocious reflexion, reducing it to 5%–10% (Table 1). However, *lin-42(RNAi)* partially suppressed the *dre-1;daf-12* delayed Mig phenotype at the L3m, increasing reflexion from 4% to 34%. Thus, these loci showed mutual suppression, suggesting that *dre-1* and *daf-12* work partially downstream or parallel to *lin-42*.

### *dre-1* Encodes an F Box Protein

*dre-1* was mapped to the center of chromosome V. By three factor, deletion, and snipSNP mapping, we localized the locus to an ~500 kb region. Rescue of mutant phenotypes was obtained with YAC Y40G12 (Figure 3A), and sequencing of genes in the region revealed mutations in K04A8.6/ceFBXO11. Based on the cDNA sequence, K04A8.6 encoded a predicted 937 aa protein highly conserved in evolution that has 57%–59% overall identity to fly, mouse, and human orthologs (Figure 3B; Figure S1). The N terminus contained an F box, a domain that interacts with SKP1-like proteins of cullin-based E3 ubiquitin ligases (Figure 3B) (Petroski and Deshaies, 2005). This was followed by three CASH domains, which are implicated in carbohydrate and sugar hydrolysis (Figure S1). The CASH domains lie within 18 predicted parallel β sheets (PBH). Additionally, this region has been proposed to have protein arginine methyltransferase activity (PRMT) in the hFBXO11 (Cook et al., 2006) and contains putative S-adenosylmethionine-binding and catalytic sites (Figure S1). However, we did not detect PRMT activity for DRE-1 or hFBXO11 (Figure S2). Finally, a Zinc finger homologous to ZnF-Ubr, involved in the N-end rule of substrate recognition and ubiquitin-mediated proteolysis (Kwon et al., 1998), was found at the C terminus. Because many heterochronic genes are targets of microRNAs, we also examined the *dre-1* 3′UTR for potential complementarity. We found 11 potential microRNA-binding sites, 3 of which were conserved in *C. briggsae dre-1*, namely, *mir-2*, *mir-59*, and *mir-71* (Figure S3).

**Table 2. Seam Cell Phenotypes**

| Genotype | % of Animals with Seam Cell Fusion Prior to L3m[a]/% of Seam Cells Exhibiting Fusion[b] | % of Animals with Adult Alae at L3m[c]/% of Seam Cells Exhibiting Adult Alae[b] | % of Animals with No Adult Alae at L4m/% of Animals with Alae Gaps |
|---|---|---|---|
| N2 | 0 | 0 | 0/0 |
| *ajm-1::gfp* | 0 | 0 | 0/0 |
| *dre-1(dh99)* | 85/52 | 15/67 | 0/45 |
| *dre-1(dh99)* post dauer | nd | nd | 0/0 |
| *dre-1(dh99)* on L4440 | 80 | 20/67 | nd |
| *dre-1(RNAi)* | 70[d]/54 | 10 | 0/83 |
| *dre-1(dh99)* on *dre-1(RNAi)* | 90[e]/nd | nd | 15/95 |
| *dre-1(dh99)/sDf36* | nd | nd | 18/nd |
| *dre-1(dh99) dre-1::gfp (dhEx452)* | 6/nd | nd | nd |
| *dre-1(dh99) dre-1(ΔF-box)::gfp (dhEx453)* | 85/nd | nd | nd |
| *lin-29(n546)*[f] | 0 | 0 | 100 |
| *lin-29(n546);dre-1(dh99)*[f] | 0 | 0 | 100 |
| *let-7(n2853)*[g] | 0 | nd | 100/100 |
| *let-7(n2853);dre-1(dh99)*[g] | 60 | nd | 20/81 |
| *lin-46(ma164)*[h] | 0 | nd | 0/100 |
| *lin-46(ma164);dre-1(dh99)*[h] | 0 | nd | 0/0 |
| *daf-12(rh61rh411)* | 0 | 0 | 0/0 |
| *daf-12(rh61rh411);dre-1(dh99)* | nd | nd | 0/56 |
| *daf-12(RNAi);dre-1(dh99)* | 58 | nd | nd |
| *lin-4(e912)*[i] | 0 | 0 | 100 |
| *lin-4(e912);dre-1(dh99)*[i] | 0 | 0 | 100 |
| N2 on *lin-41(RNAi)* | nd | 100/27 (+++)[j] | nd |
| *lin-41(RNAi);dre-1(dh99)* | nd | 100/100 (++++)[j] | nd |
| N2 on *hbl-1(RNAi)* | nd | 97/76 (++, +++)[j] | nd |
| *hbl-1(RNAi);dre-1(dh99)* | nd | 100/93 (+++)[j] | nd |

n = 20; nd not determined. One side of each animal was scored by DIC. Animals were grown at 20°C unless indicated.
[a] The percentage of animals with any precocious fusion of the seam cells prior to the L3m was determined by using the *ajm-1::gfp* marker.
[b] Among affected animals.
[c] Percentage of animals with any adult alae.
[d] A total of 14% of the animals had morphologically abnormal seam cells.
[e] A total of 53% of the animals had morphologically abnormal seam cells.
[f] A total of 100% of the animals had a protruding vulva.
[g] Animals were grown at 25°C.
[h] Animals were grown at 15°C.
[i] A total of 100% of the animals had absent vulva.
[j] Precocious alae quality: high, (++++); good, (+++); low, (++); poor, (+).

### *dre-1* Lesions

The sequences of the *dre-1* mutations revealed that all were located in the C terminus (Figure 3B) and gave penetrant Syn-Mig phenotypes (Table 1; Table S1). Remarkably, five mutations (*dh99*, *dh190*, *dh292*, *dh278*, *dh284*) pinpointed conserved glycine residues within the PBH domains. These mutations resulted in alae gap phenotypes of varying penetrance (Table 2; Table S2). Two others (*dh172*, *dh279*) truncated the protein upstream of the ZnF, while *dh280* was a missense mutation within the ZnF itself. In particular, *dh280* and *dh279* gave no alae gap phenotype, suggesting partial or selective loss of function. However, none of the obtained alleles were null. In particular, phenotypes were enhanced when *dh99* was placed over deletion *sDf36*, e.g., increasing the number of animals with full-length alae gaps from

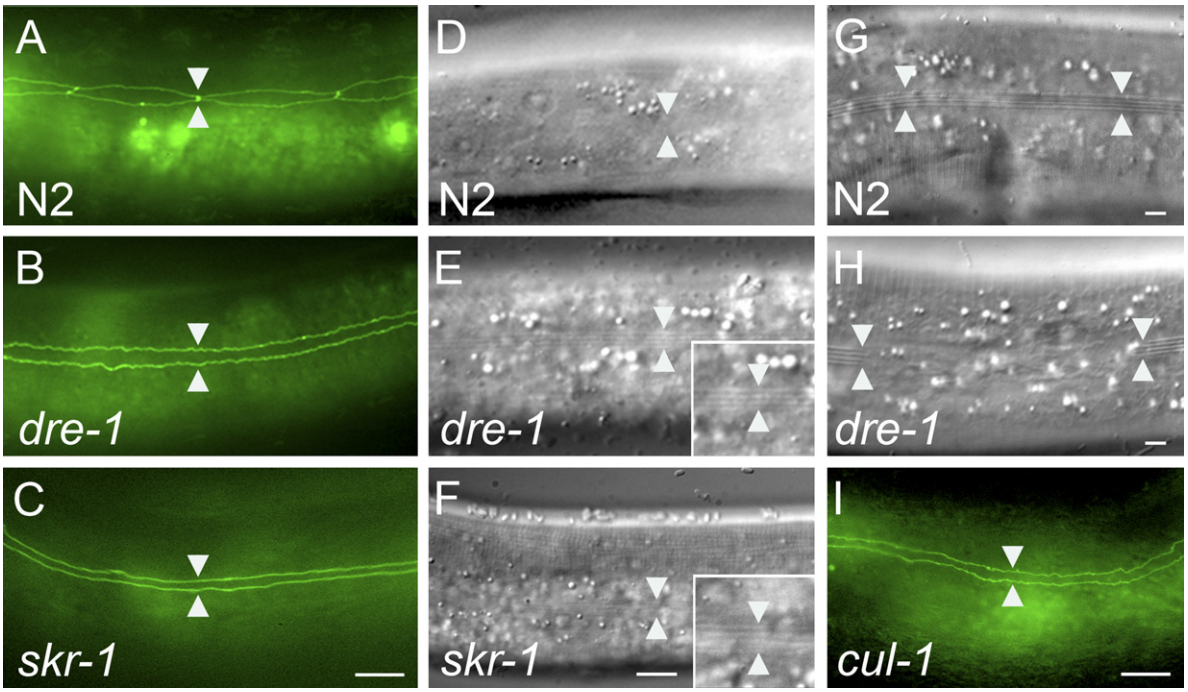


**Figure 2. Seam Cell Phenotypes**

(A) WT N2 prior to L3m; seam cells are dividing and unfused. Seam cell adherence junctions are visualized by *ajm-1::gfp* (arrowheads).
(B) *dre-1* prior to L3m; precocious seam cell fusion has occurred (arrowheads).
(C) *skr-1(RNAi)* prior to L3m; precocious seam cell fusion is shown.
(D) WT N2 L3m; no adult alae are visible.
(E) *dre-1* L3m; precocious adult alae are visible (arrowheads).
(F) *skr-1(RNAi)* L3m; precocious adult alae are shown (arrowheads).
(G) WT N2, L4m; normal adult alae are shown.
(H) *dre-1* L4m; gapped adult alae are shown (arrowheads).
(I) *cul-1(RNAi)* prior to L3m; precocious seam cell fusion is shown.
Scale bars are 10 μm.

0% to 18% (Table 2). To generate a null allele, we screened mutagenized libraries for a deletion in K04A8.6, and we obtained *hd60*, which deletes 1262 bp encompassing exons 1–3 (Figure 3B). This allele removes 110 bp of promoter and the F box domain. Ending prematurely in a stop codon, it likely encodes a molecular null.

### *dre-1* Functions in Late Embryogenesis and Ecdysis

*dre-1* null mutants displayed more severe phenotypes. Most animals (98%, n = 100) arrested as three-fold embryos that failed to hatch from their eggshells. Those that hatched arrested in L1 (Figures S4A and S4B). Defects were pleiotropic; many animals were uncoordinated and misshapen, revealing that *dre-1* works during embryogenesis. To further characterize *dre-1* loss-of-function phenotypes, we administered *dre-1(RNAi)* to wild-type and *dre-1* mutants. Consistent with a null allele, *hd60* mutant phenotypes were not enhanced by RNAi feeding or injection (data not shown). By contrast, *dre-1(dh99)* fed *dre-1* (*RNAi*) elicited stronger phenotypes, enhancing the gonadal Mig defects (Table 1), as well as precocious seam fusion and alae gap phenotypes (Table 2), showing that *dh99* is a partial loss of function. Interestingly, such animals also exhibited molting defects at L1m–L4m (Figures S4C and S4D), with greatest penetrance at the L3m and L4m (18% and 16%, n > 23, respectively). They also often displayed ruptures at the vulva and rectum, and were dumpy. These phenotypes suggest a role in the molt cycle.

### *dre-1* Expression Pattern

To determine the *dre-1* expression pattern, we constructed a full-length *gfp* fusion, consisting of a 12.3 kb promoter region fused to N-terminal *gfp*, followed by 4 kb of genomic DNA comprising the coding region and the 3′UTR. This construct was functional, as judged by its ability to rescue the precocious seam cell fusion phenotype of *dh99* or the larval lethality of *hd60* in two lines (e.g., *dhEx443* and *dhEx452*). By contrast, five different lines containing an in-frame deletion of the F box fused to *gfp* failed to rescue precocious seam cell fusion (e.g., *dhEx453*, Table 2) despite good expression, highlighting the importance of this motif for *dre-1*'s heterochronic function. Generally, DRE-1::GFP was localized to both the nucleus and cytoplasm, and it was broadly expressed, including in phenotypically affected tissues. First detected by midembryogenesis,

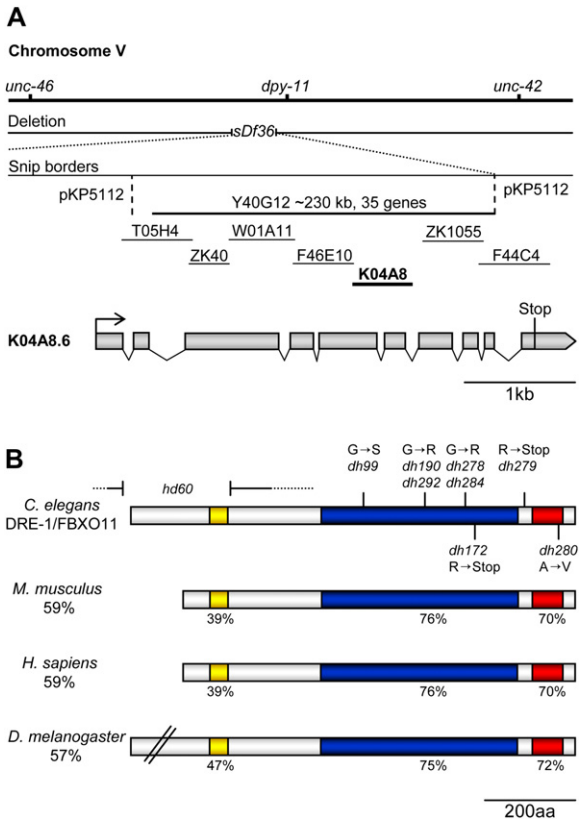


**Figure 3. Structure of the *dre-1* Locus, Gene, and Protein**

(A) *dre-1* locus. *dre-1* maps to the center of Chromosome V. Genetic markers, deletions, snipSNPs, and rescuing YAC Y40G12 are indicated below the genetic map. K04A8.6 encodes *dre-1*. The exon structure is based on existing cDNAs.

(B) Domain structure, mutations, and multiple sequence alignment of DRE-1 and FBXO11 homologs. F –box, yellow; PBH domains, blue; ZnF domain, red.

C.e., *C. elegans* DRE-1 (NP_504661); M.m., *Mus musculus* FBXO11 (Q7TPD1); H.s., *Homo sapiens* FBXO11 (NP_079409); D.m., *Drosophila melanogaster* CG9461-PA (NP_649954).

expression was most prominent in epidermal and intestinal cells (Figure 4E). By the 1.5-fold stage of embryogenesis, expression was additionally detected in neurons and other cells. During larval and adult stages, DRE-1::GFP was most visible in epidermal seam cells and hypodermis. Consistent with DRE-1's heterochronic role, expression was high in larvae and low in adults (Figures 4A and 4B). In addition, DRE-1 was strongly expressed in the P epidermal blast cells and descendents that give rise to the vulva (Figure 4C). Weak expression was seen in the somatic gonad, including the gonadoblasts, the anchor cell, dtcs, and occasionally adult spermatheca and uterus. Notably, with another construct (*dhEx346*, 4 kb promoter, 4 kb coding region), dtc expression was stronger and commenced by mid-L3 (Figure 4D). In the musculature, DRE-1 was seen in the pharynx, anal depressor, sex muscles, and body wall muscles (Figure 4D; data not shown). Finally, DRE-1 was detected in neurons of the head, tail, ventral cord, and periphery (Figure 4D; data not shown).

## Genetic Evidence that DRE-1 Works in an SCF Complex

SCF E3 ubiquitin ligase complexes are typically comprised of a cullin scaffold protein, a SKP1-like adaptor that recruits the F box substrate recognition component, and the RBX ring finger that bridges to the E2 ubiquitin conjugating enzyme (Petroski and Deshaies, 2005). To test the hypothesis that DRE-1 works in such a complex, we screened cullins (4 of 6 genes), *skp1*-related genes (*skrs*, 15 of 23 genes), and *rbx1* homologs (2 genes) by RNAi knockdown. We examined animals for *dre-1*-like defects, scoring precocious seam cell fusion and adult alae gap phenotypes in wild-type and Syn-Mig phenotypes in *daf-12* null mutants. From such a screen, *skr-1* and *cul-1* produced visible precocious seam cell fusion, alae gap, and Syn-Mig phenotypes (Figures 2C, 2F, and 2I; Table S3). Moreover, like RNAi of *dre-1*, RNAi of *skr-1* and *cul-1* enhanced the phenotypes of *dre-1(dh99)*, revealing more penetrant molting defects (data not shown). In addition, double RNAi of *rbx-1* and *rbx-2* also induced precocious fusion of the seam cells, and RNAi of *rbx-1* alone induced alae gap phenotypes (Table S3). Altogether, phenotypic congruence suggests that DRE-1, SKR-1, CUL-1, and RBX-1/2 could work in a complex to influence developmental timing.

## DRE-1 Acts in an SCF Complex

F box proteins interact with SKP1 in SCF ubiquitin ligase complexes through their F box motif (Petroski and Deshaies, 2005). To test the idea that DRE-1 and SKR-1 form a complex, we examined them for physical interaction. First, we looked in the yeast two-hybrid system. Using full-length DRE-1, we detected physical interaction with SKR-1 (Figure 5A) and its close relative SKR-2 (data not shown), as judged by prototrophy on −histidine and −uracil media. By contrast, no interaction was seen with SKR-10, or with any of the other SKR proteins tested (see Supplemental Experimental Procedures). As expected, interaction was dependent on the N-terminal half containing the F box (data not shown).

Next, we tested whether DRE-1 and SKR-1 associated by coimmunoprecipitation in mammalian cell culture. Flag-tagged *dre-1* and Myc-tagged *skr-1* were transfected into COS7 cells, lysates were subjected to immunoprecipitation with anti-Flag Ab, and a western blot was probed with anti-Myc Ab. We found that DRE-1 effectively coprecipitated SKR-1 when both were transfected, while the singly transfected controls yielded no signal (Figure 5B). Additionally, an in-frame deletion lacking the F box (DRE-1ΔF-box) did not precipitate SKR-1, despite being highly expressed, revealing that interaction relies on this motif. Finally, we asked whether the human orthologs coprecipitated in cell culture. Indeed, Flag-tagged hFBXO11 brought down both endogenous SKP1 and CUL1 in coimmunoprecipitation experiments in HEK293T cells (Figure 5C), showing that the complex of these proteins is conserved in evolution. Moreover, hFBXO11 bound most avidly to neddylated CUL1, the presumed activated form in the SCF complex (Chiba and Tanaka, 2004).

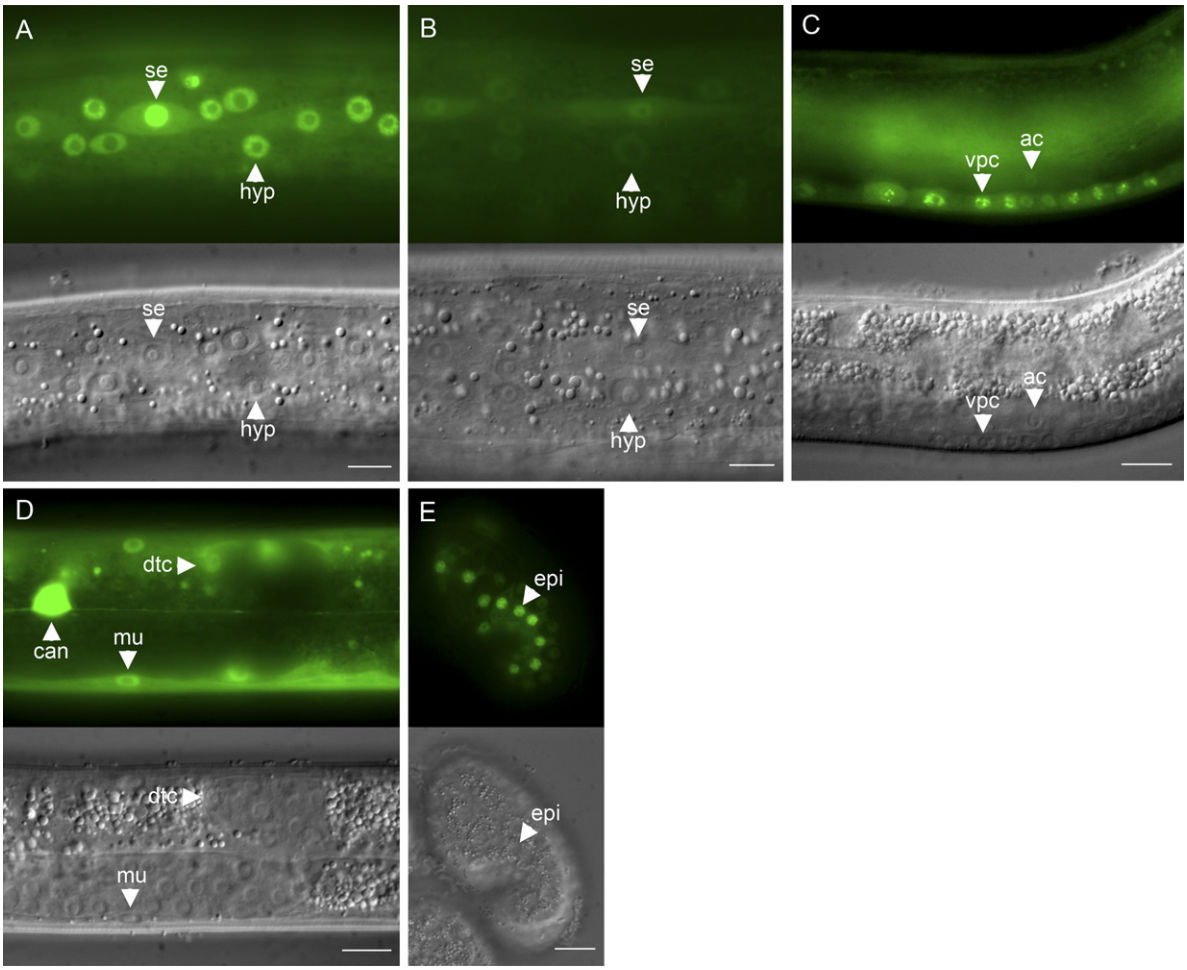


**Figure 4. *dre-1::gfp* Expression Pattern**

(A) Seam (se) and hypodermal (hyp) cells (mid-L3).

(B) Seam (se) and hypodermal (hyp) cells (adult).

(C) Vulval cells (vpc, all cells aligned in a row are vulva precursor cells) and anchor cell (ac) (mid-L3).

(D) Distal tip cells (dtcs), body wall muscle cell (mu), and CAN neuron (around the L3m) (*dhEx346*).

(E) Epidermal cell (epi) embryo.

Nomarski images are shown beneath each *gfp* image. (A)–(C) and (E) show the *dhEx453 gfp* transgene; (D) shows the *dhEx346 gfp* transgene. The scale bars are 10 μm.

The epistasis data described above suggested that LIN-29 could be a potential target of DRE-1 regulation. If so, then LIN-29 is predicted to be expressed precociously in the seams during L3 in the *dre-1* background. Accordingly, we observed that weak LIN-29 expression in seam cells, as visualized with anti-LIN-29 Ab, appeared precociously by mid-L3 in *dh99* in 8.7% of animals (n = 138), but not in wild-type (n = 105) (Figure 5D). As reported, LIN-29 was only detected in the seam cells by early L4 in wild-type (Bettinger et al., 1996). Thus, DRE-1 may either directly or indirectly regulate LIN-29 protein level. To test whether DRE-1 directly targets LIN-29, we measured the ability of the two proteins to specifically associate in HEK293T cells. For these experiments, we cotransfected HA-tagged *lin-29* and Flag-tagged *dre-1*. Despite strong expression of the input proteins, we found that LIN-29 immunoprecipitated by anti-HA Ab failed to coprecipitate DRE-1, hFBXO11, or β-TRCP (Figure S5), suggesting that it may not be a direct target.

## DISCUSSION

In this work, we identified a phyletically ancient F box protein, DRE-1, as a central component of the heterochronic hierarchy. DRE-1 resides within an SCF E3 ubiquitin ligase complex, as does its human counterpart, hFBXO11. Thus, this study implies an important dimension of control within the heterochronic circuit: SCF-mediated protein modification or proteolysis. Remarkably, of the numerous F box proteins found in metazoan genomes, only six are conserved in worms, flies, mice, and men, and DRE-1 is among these (Jin et al., 2004). Moreover, only 5 of the

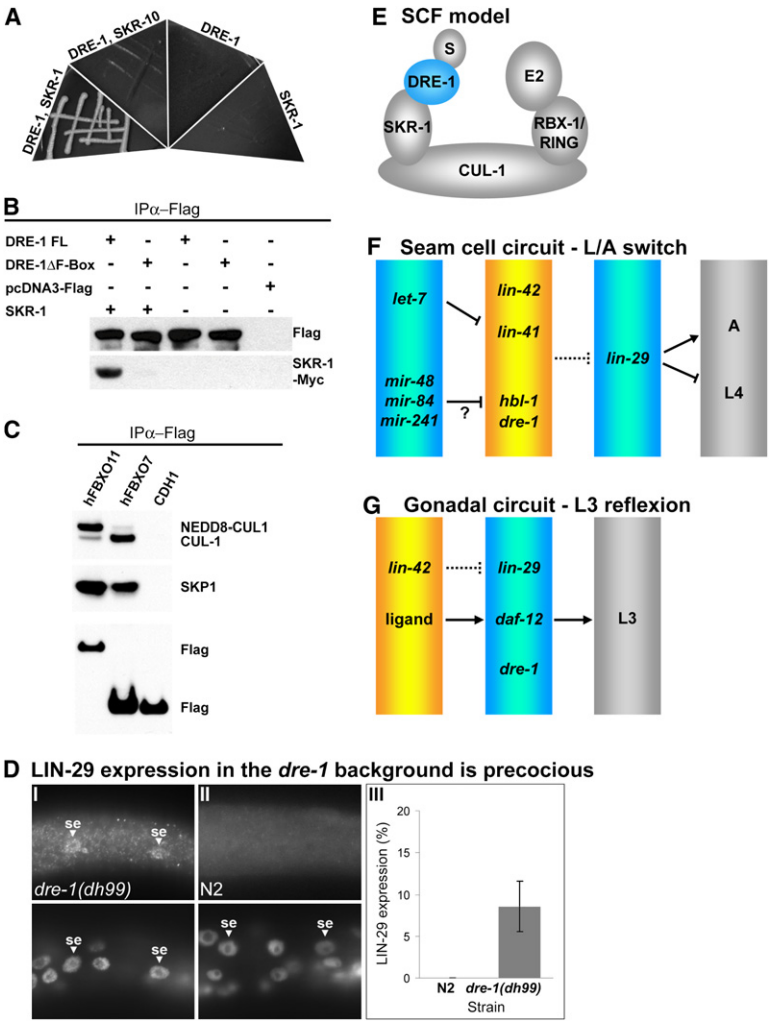


**Figure 5. DRE-1 Is Part of an SCF Complex and Acts in the Heterochronic Circuit**

(A) Yeast two-hybrid interaction between DRE-1 and SKR-1. From left to right: *dre-1*, *skr-1*; *dre-1*, *skr-10*; *dre-1*; *skr-1*. *dre-1* and *skr-1*, but not *skr-10*, grew on −TRP−LEU−HIS−URA plates, indicating interaction. Control plates for growth without interaction were −TRP−LEU (data not shown).

(B) Coimmunoprecipitation of *C. elegans* DRE-1-Flag and SKR-1-Myc from COS7 cells. DRE-1-Flag tag was immunoprecipitated with anti-Flag antibody, and western blots were probed with anti-Myc antibodies. *skr-1* was cotransfected with *dre-1* constructs in lanes 1, 2, and 5. Equal expression levels of proteins were verified by western blot analysis (data not shown). DRE-1FL (full length), DRE-1Δ F-box (F box deletion), and SKR-1 (full length).

(C) Coimmunoprecipitation of hFBXO11-Flag and endogenous SKP1 and CUL1 from HEK293T cells. hFBXO11-Flag was immunoprecipitated with anti-Flag antibody, and western blots were probed with anti-SKP1 and anti-CUL1 antibodies. hFBXO11 mainly binds the NEDD8-conjugated, active form of CUL1. In contrast, hFBX07 mostly binds unconjugated CUL1. Negative-control CDH1 (E-cadherin) fails to bind CUL1.

(D) LIN-29 expression precocious in the *dre-1* mutants. (I) *dre-1(dh99)*. Precocious expression of LIN-29 in seam (se) cells in mid-L3, stained with anti-LIN-29 Ab. (II) N2. No expression of LIN-29 in seam (se) cells in mid-L3. DAPI staining of nuclei is shown below Ab staining. The scale bar is 10 μm. (III) Percentage of animals with precocious LIN-29 expression by mid-L3. Wild-type N2, 0% (0/105); *dre-1(dh99)*, 8.7% (12/138). Data are from three experiments. Error bars illustrate standard deviation of the mean.

(E) SCF model.

(F) Seam cell circuit, L/A transition. For late larval programs, *dre-1*, *hbl-1*, *lin-41*, and *lin-42* work together to prevent *lin-29* expression. At the L/A switch, expression of *let-7* and *let-7* sisters downregulates *lin-41* and *hbl-1*, leading to *lin-29* derepression. *lin-29* could be regulated by transcription (*lin-42*, *hbl-1*), translation (*lin-41*), and protein stability (*dre-1*). Genes of the early timer are not shown.

(G) Gonadal circuit, L3 reflexion. During L2, *lin-42* inhibits *lin-29*, while unknown factors may inhibit *dre-1* and *daf-12*. During L3, *dre-1*, liganded *daf-12*, and *lin-29* together promote gonadal reflexion.

68 SCF ligases in human have clearly ascribed functions to date. Therefore, the functional depiction of DRE-1 in the worm may shed light on physiologic roles of homologs in higher animals.

## *dre-1* Is a Heterochronic Gene

Several lines of evidence argue that *dre-1* is a heterochronic locus. First, mutants exhibit precocious development in epidermal seam cells, giving rise to seam cell fusion and adult cuticular alae formation one full stage earlier than normal. These phenotypes suggest that *dre-1(+)* normally specifies late larval development by preventing early expression of adult programs. Accordingly, *dre-1::gfp* expression in the epidermis was high during larval stages and declined in adult. Second, interactions with other heterochronic loci suggest that it works in the L/A switch, upstream of the *lin-29*/ZnF protein and downstream or parallel to *let-7*/microRNA (Figure 5F). Because the *dre-1* 3′UTR lacks *let-7*-binding sites, it is unlikely a direct *let-7* target. Like many genes that work in the L/A switch, *dre-1* precocious phenotypes were impenetrant. *dre-1* was dramatically enhanced by *lin-41*/RBCC, but not by *hbl-1*/hunchback. These interactions may indicate that *dre-1* works in parallel to *lin-41* and perhaps in the same pathway as *hbl-1* (Figure 5F). It seems probable that regulation of the L/A switch occurs simultaneously at the levels of transcription, mRNA stability, translational efficiency, and protein stability to ensure robust control. Different tiers of regulation might explain the existence of distinct parallel genetic pathways governing this developmental choice. Despite working earlier in development, *lin-4* is epistatic to *dre-1*, presumably because it works

through these parallel pathways, masking *dre-1*'s downstream position. Conceivably, *dre-1* may also function earlier in the L2/L3 transition, too, since *lin-46*/gephyrin suppressed *dre-1* precocious phenotypes, but this issue must be further investigated.

Third, *dre-1* has a role in gonadal heterochrony, promoting L3 reflexion of the dtcs. As in the seam cells, *dre-1* represents one branch of parallel pathways that govern this process. Notably, *dre-1;daf-12*, *dre-1;lin-29*, and *daf-12;lin-29* double mutants exhibited a penetrant Syn-Mig phenotype, in which the dtcs failed one or both of their L3 turns. A further enhancement was seen in the triple mutant. The Syn-Mig defect is attributed to delayed heterochrony, in which the dtcs either fail to advance to L3 and/or repeat L2 programs of longitudinal migration. These results suggest that regulation by transcription (*daf-12*, *lin-29*) and perhaps protein stability (*dre-1*) is important for gonadal reflexion. Moreover, *dre-1* gave similar Syn-Mig phenotypes with mutants deficient in production of the DAF-12 ligand, suggesting that gonadal reflexion is hormone dependent (Figure 5G).

*lin-42(+)* regulates dtc migration also, since *lin-42(RNAi)* induces precocious dtc reflexion at the L2m. *lin-29* completely suppressed this phenotype (Tennessen et al., 2006), suggesting that *lin-42(+)* prevents precocious reflexion by inhibiting *lin-29* during the L2 stage. Similarly, *dre-1*, *daf-12*, and *dre-1;daf-12* delayed Syn-Mig mutants suppressed *lin-42* phenotypes at the L2m, although not completely. Moreover, *lin-42(RNAi)* partially restored gonadal reflexion of *dre-1;daf-12* at the L3m. This mutual suppression suggests that *dre-1*/*daf-12* work downstream or parallel to *lin-42* in a regulatory pathway (Figure 5G). Further work should elucidate how these and other factors govern gonadal timing. Regulation of *dre-1* itself could occur on several levels. Notably, the presence of potential microRNA-binding sites in its 3′UTR, three of which are conserved in *C. briggsae*, suggests that *dre-1* could be posttranscriptionally/translationally regulated (Figure S3).

Curiously, *dre-1(+)* may function to prevent the L/A transition in the seam, but may function to facilitate this transition in the gonad, perhaps reflecting tissue differences in the way circuits are organized. Such janus-like behavior is not without precedent, since *daf-12* mutants reportedly display delayed and precocious phenotypes in seam cells at L2m and L3m, respectively (Antebi et al., 1998; Grosshans et al., 2005). Importantly, *dre-1* simultaneously influences several temporal events in different tissues, arguing for a regulatory rather than a structural role in the processes of cell division, fusion, or migration per se. It should be mentioned that we interpret the regulatory order derived from the genetic interactions as tentative working hypotheses, as some of the mutants used for analysis were non-null, the heterochronic circuit has parallel activities, and many components function at multiple steps.

Recently, two mouse mutants, *Mutt* and *Jeff*, have been shown to harbor mutations in the murine FBXO11 and to display facial clefting and perinatal lethality (Hardisty-Hughes et al., 2006). Conceivably, some of these abnormalities could result from defects in developmental timing. Additionally, *Jeff* mutants develop otitis media, an inflammation of the ear leading to hearing impairment. Intriguingly, the *hfbxo11* mRNA expression is downregulated in the depigmentation disease vitiligo (Le Poole et al., 2001), which is thought to arise from an autoimmune condition. Thus, FBXO11 homologs may additionally play a role in inflammation and immunity.

### Chronological and Developmental Age

Like other heterochronic regulators (e.g., *hbl-1* [Fay et al., 1999]), *dre-1* evidently has other physiological roles, including responsibilities in late embryogenesis, hatching, and larval molting. Notably, *dre-1* affects all four larval molts, while most other heterochronic loci only affect the final molt, causing premature or delayed termination of the molt cycle due to heterochronic expression of *lin-29*, which mediates this process (Ambros, 1989). Both hatch and ecdysis can be seen as measures of chronological age that mark elapsed stages. Conceivably, *dre-1* is a key regulator of both chronological (hatch, the molt cycle) and developmental age (the heterochronic timer), identifying the first gene that broadly perturbs both. Generally, ubiquitin-mediated modification and proteolysis have been shown to regulate other biological timers, such as the cell cycle or circadian clock (Petroski and Deshaies, 2005). Stage-counting mechanisms may also rely on protein modification and degradation for proper advance. Whether *dre-1*'s role in heterochronic and molting timers are independent or functionally interlinked is unknown.

### DRE-1 Is Part of an SCF Complex

*dre-1*'s molecular identity as an F box protein suggests that it works in an SCF E3 ubiquitin ligase complex (Figure 5E) (Jin et al., 2004). It also contains putative PRMT motifs, and it may thus work as an arginine methyltransferase. Our work here clearly points to the importance of the SCF complex. First, an in-frame deletion mutant lacking the F box was unable to rescue the precocious seam fusion phenotype, showing this region to be essential to the heterochronic function of *dre-1*. Second, knockdown of the *C. elegans* cullin, *cul-1*, and the *skp1*-like homolog, *skr-1*, resulted in similar heterochronic defects as *dre-1*, namely, precocious fusion of epidermal seam cells, gaps in adult alae, and Syn-Mig phenotypes with the *daf-12* null. Such phenotypes were specific, as they were not seen with the knockdown of other cullins or *skr* genes. Phenotypic congruence strongly suggests that these proteins work together in a unified biological process. Accordingly, DRE-1 associated with SKR-1 through its F box motif, in both yeast two-hybrid and coimmunoprecipitation experiments. Strikingly, the human homologs hFBXO11 and SKP1 coimmunoprecipitated in cell culture, revealing that this interaction is evolutionarily conserved. In addition, hFBXO11, SKP1, and CUL1 assemble in an SCF complex in which CUL1 is found in its NEDD8-conjugated, active form. Homologs of the RBX ring finger, another core component of the SCF complex, also showed precocious fusion of the seam cells. However, heterochronic

phenotypes were not wholly penetrant in the seams and were absent from the gonad, suggesting that other ring finger proteins could subsume this function.

Of critical interest are DRE-1 targets, their mode of recognition, and their regulation. Notably, most *dre-1* lesions clustered in the C-terminal PBH and ZnF-Ubr domains, indicating that these regions as critical to function. A similar ZnF-Ubr domain in N-recognin confers substrate recognition in the N-end rule pathway of ubiquitin-mediated proteolysis (Kwon et al., 1998), and it may have a similar function in DRE-1. The PBH repeats comprise the so-called CASH domains, which are implicated in carbohydrate binding and hydrolysis, suggesting specific recognition of glycosylated or ribosylated substrates. Interestingly, the PBH repeats are proposed to fold into a β propeller (Cook et al., 2006), which is reminiscent of the WD40 propeller domain in β-TRCP F box protein and other FBWs (Cardozo and Pagano, 2004). DRE-1 and homologs also contain diverged signature motifs of PRMTs embedded within the PBH domains, and hFXBO11 is proposed to have PRMT activity (Cook et al., 2006). However, we did not detect PRMT activity with DRE-1 (immunoprecipitated from cells by HA tag) or with GST-purified DRE-1 and hFBXO11 (Figure S2), though it is possible that this activity is present in vivo.

Since SCF complexes trigger targeted proteolysis, it seems most likely that DRE-1 covalently modifies or targets key developmental proteins for degradation. A simple hypothesis is that DRE-1 erases cellular memories of developmental age, or that it fine-tunes protein activity at the level of stability. DRE-1 targets would be expected to behave as *dre-1* suppressors. Because *dre-1* loss should lead to an accumulation of substrates, compensatory reduction of those substrates is expected to restore normal function. Such behavior has been observed in *C. elegans* Notch signaling and synaptogenesis (Hubbard et al., 1997; Liao et al., 2004). The most obvious direct target in the L/A switch is LIN-29, since the mutant shows strict epistasis within epidermal seam cells. Consistent with a regulatory target, LIN-29 was expressed precociously in *dre-1* mutants. However, physical interaction between DRE-1 and LIN-29 was undetected, either by the yeast two-hybrid experiments (N.F. and A.A., unpublished data) or by coimmunoprecipitation in cell culture (Figure S5). Regulation of LIN-29 may therefore be indirect or require specific modifications for recognition not present in these assays. At this point, it seems less likely that its substrates include any of the currently known heterochronic regulators. Presumably, an analysis of *dre-1* suppressors will likely identify novel targets within the heterochronic pathway.

In sum, the placement of DRE-1 within the heterochronic circuit suggests a key physiologic role in differentiation and temporal programming. Given DRE-1's striking evolutionary conservation, as well as the conservation of most components of the heterochronic circuit, what is learned in the worm may contribute to an understanding of how mammalian developmental timing and other processes are orchestrated.

## EXPERIMENTAL PROCEDURES

### Mutant Isolation and Syn-Mig Phenotypes

*dre-1* mutants were isolated in F2 mutant screens for enhancement of the heterochronic gonadal migration (Mig) phenotype of the *daf-12(rh61rh411)* mutant after 0.5% ethylmethanesulfonate treatment. Scoring of 127,000 genomes for Mig phenotypes yielded 8 *dre-1* alleles (*dh99*, *dh172*, *dh190*, *dh278*, *dh279*, *dh280*, *dh284*, *dh292*) and 1 allele of *dre-2(dh184)*. Over half of the Syn-Mig mutants were sterile and were not recovered. Mutants were outcrossed three times. The following mutants were examined for synergistic Mig phenotypes in conjunction with *dre-1(dh99)* and *daf-12(rh61rh411)*: *lin-29(n546)*, *let-7(n2853ts)*, *lin-46(ma164)*, *lin-4(e912)*, *daf-9(k182)*, *daf-36(k114)*, *lin-28(n719)*, *lin-14(ma135)*, *lin-41(n2914)*, *hbl-1(RNAi)*, *tim-1(RNAi)*, and *kin-20(RNAi)*.

### Positional Cloning of *dre-1*

*dre-1* was mapped to chromosome V by snipSNP mapping (Wicks et al., 2001). *unc-46(e177);dpy-11(e224)* and *dpy-11(e224);unc-42(e270)* were used for three-factor mapping. For fine snipSNP mapping, the triple mutant *dpy-11(e224);dre-1(dh99);unc-42(e270)* was used to select for recombinants, and snipSNPs were analyzed. YACs (100–200 ng/ml) and cosmids (5–15 ng/ml) were microinjected into *dre-1(dh99)* to assay mutant rescue.

### Construction of *dre-1::gfp* Strains and *dre-1* Deletion

For *dre-1::gfp*, a 4 kb promoter was amplified with primers 5′-GGTACCCGAGGGGACATCGAGATAG-3′ and 5′-GGTACCTTCCTGG CCAACCAGAGAC-3′ and was cloned into Fire vector L3781 (BA 279). The *dre-1* ORF and the *dre-1* 3′UTR region were amplified with primers 5′-GCTAGCATGTCGTCCTCTTCGTCAC-3′ and 5′-ACTAGTTACTTAC TCCACTCCACACAG-3′ and were cloned into BA279 (BA280). Lines containing this construct included *dhEx346* and *dhIs442*. To obtain the full-length promoter construct, we substituted the promoter from BA279 with a 12.3 kb promoter by using primers 5′-GCGGCCGCGT TGCACACAAAACATTATTATTTTCTTTCTCTT-3′ and 5′-TACGTATCT CGTCCCTGAGATCTCTCATTT-3′ (BA508). Resulting lines containing this array included *dhEx443* and *dhEx452*. For the *dre-1ΔF-box* construct, nucleotides 484–621 were removed from the genomic *dre-1* locus. Resulting lines containing this array included *dhEx453*, *dhEx454*, *dhEx455*, *dhEx456*, and *dhEx457*. *dre-1(hd60)* was isolated by PCR screening through pooled mutagenized libraries for deletion in the locus. *dre-1(hd60)* deleted 1262 bp, removing exons 1–3.

### Supplemental Data

Supplemental Data include tables of additional Mig and seam cell phenotypes, figures of *dre-1* multiple sequence alignment, PRMT assays, potential miRNA-binding sites, other phenotypes of *dre-1*, DRE-1/LIN-29 interaction studies, and Supplemental Experimental Procedures and are available at http://www.developmentalcell.com/cgi/content/full/12/3/443/DC1/.

## ACKNOWLEDGMENTS

We are indebted to Ann Rougvie for *lin-42* RNAi constructs and LIN-29 Ab, Edward Kipreos for two-hybrid constructs, the *Caenorhabditis* Genetics Center for worm strains, Yuji Kohara for cDNAs, the Sanger Center for cosmids, and Andy Fire for GFP vectors. We would also like to thank the laboratory of Tae Ho Shin for technical help, and Zheng Zhou for manuscript comments. This work was supported by National Instituets of Health (A.A., M.P.), the Emerald Foundation (D.G.), and the Max Planck Gesellschaft (A.A., N.F., K.N.).

Received: May 7, 2006
Revised: January 20, 2007
Accepted: January 26, 2007
Published: March 5, 2007

## REFERENCES

Abbott, A.L., Alvarez-Saavedra, E., Miska, E.A., Lau, N.C., Bartel, D.P., Horvitz, H.R., and Ambros, V. (2005). The *let-7* MicroRNA family members *mir-48*, *mir-84*, and *mir-241* function together to regulate developmental timing in *C. elegans*. Dev. Cell *9*, 403–414.

Abrahante, J.E., Daul, A.L., Li, M., Volk, M.L., Tennessen, J.M., Miller, E.A., and Rougvie, A.E. (2003). The *C. elegans* hunchback-like gene *lin-57/hbl-1* controls developmental time and is regulated by microRNAs. Dev. Cell *4*, 625–637.

Ambros, V. (1989). A hierarchy of regulatory genes controls a larva-to-adult developmental switch in *C. elegans*. Cell *57*, 49–57.

Ambros, V., and Horvitz, H.R. (1984). Heterochronic mutants of the nematode *C. elegans*. Science *226*, 409–416.

Antebi, A., Culotti, J.G., and Hedgecock, E.M. (1998). *daf-12* regulates developmental age and the dauer alternative in *C. elegans*. Development *125*, 1191–1205.

Antebi, A., Yeh, W.H., Tait, D., Hedgecock, E.M., and Riddle, D.L. (2000). *daf-12* encodes a nuclear receptor that regulates the dauer diapause and developmental age in *C. elegans*. Genes Dev. *14*, 1512–1527.

Banerjee, D., Kwok, A., Lin, S.Y., and Slack, F.J. (2005). Developmental timing in *C. elegans* is regulated by *kin-20* and *tim-1*, homologs of core circadian clock genes. Dev. Cell *8*, 287–295.

Bettinger, J.C., Lee, K., and Rougvie, A.E. (1996). Stage-specific accumulation of the terminal differentiation factor LIN-29 during *C. elegans* development. Development *122*, 2517–2527.

Cardozo, T., and Pagano, M. (2004). The SCF ubiquitin ligase: insights into a molecular machine. Nat. Rev. Mol. Cell Biol. *5*, 739–751.

Chalfie, M., Horvitz, H.R., and Sulston, J.E. (1981). Mutations that lead to reiterations in the cell lineages of *C. elegans*. Cell *24*, 59–69.

Chiba, T., and Tanaka, K. (2004). Cullin-based ubiquitin ligase and its control by NEDD8-conjugating system. Curr. Protein Pept. Sci. *5*, 177–184.

Cook, J.R., Lee, J.H., Yang, Z.H., Krause, C.D., Herth, N., Hoffmann, R., and Pestka, S. (2006). FBXO11/PRMT9, a new protein arginine methyltransferase, symmetrically dimethylates arginine residues. Biochem. Biophys. Res. Commun. *342*, 472–481.

Fay, D.S., Stanley, H.M., Han, M., and Wood, W.B. (1999). A *C. elegans* homologue of hunchback is required for late stages of development but not early embryonic patterning. Dev. Biol. *205*, 240–253.

Gerisch, B., Weitzel, C., Kober-Eisermann, C., Rottiers, V., and Antebi, A. (2001). A hormonal signaling pathway influencing *C. elegans* metabolism, reproductive development, and life span. Dev. Cell *1*, 841–851.

Grosshans, H., Johnson, T., Reinert, K.L., Gerstein, M., and Slack, F.J. (2005). The temporal patterning microRNA *let-7* regulates several transcription factors at the larval to adult transition in *C. elegans*. Dev. Cell *8*, 321–330.

Hallam, S.J., and Jin, Y. (1998). *lin-14* regulates the timing of synaptic remodelling in *C. elegans*. Nature *395*, 78–82.

Hardisty-Hughes, R.E., Tateossian, H., Morse, S.A., Romero, M.R., Middleton, A., Tymowska-Lalanne, Z., Hunter, A.J., Cheeseman, M., and Brown, S.D. (2006). A mutation in the F-box gene, Fbxo11, causes otitis media in the *Jeff* mouse. Hum. Mol. Genet. *15*, 3273–3279.

Held, J.M., White, M.P., Fisher, A.L., Gibson, B.W., Lithgow, G.J., and Gill, M.S. (2006). DAF-12-dependent rescue of dauer formation in *C. elegans* by (25S)-cholestenoic acid. Aging Cell *5*, 283–291.

Hubbard, E.J., Wu, G., Kitajewski, J., and Greenwald, I. (1997). *sel-10*, a negative regulator of *lin-12* activity in *C. elegans*, encodes a member of the CDC4 family of proteins. Genes Dev. *11*, 3182–3193.

Jeon, M., Gardner, H.F., Miller, E.A., Deshler, J., and Rougvie, A.E. (1999). Similarity of the *C. elegans* developmental timing protein LIN-42 to circadian rhythm proteins. Science *286*, 1141–1146.

Jia, K., Albert, P.S., and Riddle, D.L. (2002). DAF-9, a cytochrome P450 regulating *C. elegans* larval development and adult longevity. Development *129*, 221–231.

Jin, J., Cardozo, T., Lovering, R.C., Elledge, S.J., Pagano, M., and Harper, J.W. (2004). Systematic analysis and nomenclature of mammalian F-box proteins. Genes Dev. *18*, 2573–2580.

Kwon, Y.T., Reiss, Y., Fried, V.A., Hershko, A., Yoon, J.K., Gonda, D.K., Sangan, P., Copeland, N.G., Jenkins, N.A., and Varshavsky, A. (1998). The mouse and human genes encoding the recognition component of the N-end rule pathway. Proc. Natl. Acad. Sci. USA *95*, 7898–7903.

Lagos-Quintana, M., Rauhut, R., Yalcin, A., Meyer, J., Lendeckel, W., and Tuschl, T. (2002). Identification of tissue-specific microRNAs from mouse. Curr. Biol. *12*, 735–739.

Le Poole, I.C., Sarangarajan, R., Zhao, Y., Stennett, L.S., Brown, T.L., Sheth, P., Miki, T., and Boissy, R.E. (2001). 'VIT1', a novel gene associated with vitiligo. Pigment Cell Res. *14*, 475–484.

Lee, R.C., Feinbaum, R.L., and Ambros, V. (1993). The *C. elegans* heterochronic gene *lin-4* encodes small RNAs with antisense complementarity to *lin-14*. Cell *75*, 843–854.

Li, M., Jones-Rhoades, M.W., Lau, N.C., Bartel, D.P., and Rougvie, A.E. (2005). Regulatory mutations of *mir-48*, a *C. elegans let-7* family microRNA, cause developmental timing defects. Dev. Cell *9*, 415–422.

Liao, E.H., Hung, W., Abrams, B., and Zhen, M. (2004). An SCF-like ubiquitin ligase complex that controls presynaptic differentiation. Nature *430*, 345–350.

Lin, S.Y., Johnson, S.M., Abraham, M., Vella, M.C., Pasquinelli, A., Gamberi, C., Gottlieb, E., and Slack, F.J. (2003). The *C. elegans* hunchback homolog, *hbl-1*, controls temporal patterning and is a probable microRNA target. Dev. Cell *4*, 639–650.

Liu, Z.C., and Ambros, V. (1989). Heterochronic genes control the stage-specific initiation and expression of the dauer larva developmental program in *C. elegans*. Genes Dev. *3*, 2039–2049.

Ludewig, A.H., Kober-Eisermann, C., Weitzel, C., Bethke, A., Neubert, K., Gerisch, B., Hutter, H., and Antebi, A. (2004). A novel nuclear receptor/coregulator complex controls *C. elegans* lipid metabolism, larval development, and aging. Genes Dev. *18*, 2120–2133.

Moss, E.G., Lee, R.C., and Ambros, V. (1997). The cold shock domain protein LIN-28 controls developmental timing in *C. elegans* and is regulated by the *lin-4* RNA. Cell *88*, 637–646.

Motola, D.L., Cummins, C.L., Rottiers, V., Sharma, K.K., Li, T., Li, Y., Suino-Powell, K., Xu, H.E., Auchus, R.J., Antebi, A., and Mangelsdorf, D.J. (2006). Identification of ligands for DAF-12 that govern dauer formation and reproduction in *C. elegans*. Cell *124*, 1209–1223.

Pasquinelli, A.E., Reinhart, B.J., Slack, F., Martindale, M.Q., Kuroda, M.I., Maller, B., Hayward, D.C., Ball, E.E., Degnan, B., Muller, P., et al. (2000). Conservation of the sequence and temporal expression of *let-7* heterochronic regulatory RNA. Nature *408*, 86–89.

Pepper, A.S., McCane, J.E., Kemper, K., Yeung, D.A., Lee, R.C., Ambros, V., and Moss, E.G. (2004). The *C. elegans* heterochronic gene *lin-46* affects developmental timing at two larval stages and encodes a relative of the scaffolding protein gephyrin. Development *131*, 2049–2059.

Petroski, M.D., and Deshaies, R.J. (2005). Function and regulation of cullin-RING ubiquitin ligases. Nat. Rev. Mol. Cell Biol. *6*, 9–20.

Reinhart, B.J., Slack, F.J., Basson, M., Pasquinelli, A.E., Bettinger, J.C., Rougvie, A.E., Horvitz, H.R., and Ruvkun, G. (2000). The 21-nucleotide *let-7* RNA regulates developmental timing in *C. elegans*. Nature *403*, 901–906.

Rottiers, V., Motola, D.L., Gerisch, B., Cummins, C.L., Nishiwaki, K., Mangelsdorf, D.J., and Antebi, A. (2006). Hormonal control of *C. elegans* dauer formation and life span by a Rieske-like oxygenase. Dev. Cell *10*, 473–482.

Rougvie, A.E. (2005). Intrinsic and extrinsic regulators of developmental timing: from miRNAs to nutritional cues. Development *132*, 3787–3798.

Rougvie, A.E., and Ambros, V. (1995). The heterochronic gene *lin-29* encodes a zinc finger protein that controls a terminal differentiation event in *C. elegans*. Development *121*, 2491–2500.

Ruvkun, G., and Giusto, J. (1989). The *C. elegans* heterochronic gene *lin-14* encodes a nuclear protein that forms a temporal developmental switch. Nature *338*, 313–319.

Slack, F.J., Basson, M., Liu, Z., Ambros, V., Horvitz, H.R., and Ruvkun, G. (2000). The *lin-41* RBCC gene acts in the *C. elegans* heterochronic pathway between the *let-7* regulatory RNA and the LIN-29 transcription factor. Mol. Cell *5*, 659–669.

Sulston, J.E., and Horvitz, H.R. (1977). Post-embryonic cell lineages of the nematode, *C. elegans*. Dev. Biol. *56*, 110–156.

Sulston, J.E., Schierenberg, E., White, J.G., and Thomson, J.N. (1983). The embryonic cell lineage of the nematode *C. elegans*. Dev. Biol. *100*, 64–119.

Tennessen, J.M., Gardner, H.F., Volk, M.L., and Rougvie, A.E. (2006). Novel heterochronic functions of the *C. elegans* period-related protein LIN-42. Dev. Biol. *289*, 30–43.

Wicks, S.R., Yeh, R.T., Gish, W.R., Waterston, R.H., and Plasterk, R.H. (2001). Rapid gene mapping in *C. elegans* using a high density polymorphism map. Nat. Genet. *28*, 160–164.

Wightman, B., Ha, I., and Ruvkun, G. (1993). Posttranscriptional regulation of the heterochronic gene *lin-14* by *lin-4* mediates temporal pattern formation in *C. elegans*. Cell *75*, 855–862.